



## Heat Transfer Aspects on Rotating MHD Two-phase Convective Flow through an Inclined Channel in the Presence of Electric Field

P. Sri Ramachandra Murty<sup>1\*</sup> and G. Balaji Prakash<sup>1</sup>

<sup>1</sup>Department of Mathematics, GIT, Gitam University, Visakhapatnam,  
Pin code: 530 045, India.

### Authors' contributions

*This whole work was carried out in collaboration between both authors PSRM and GBP.  
Both authors read and approved the final manuscript.*

Original Research Article

Received 17<sup>th</sup> May 2014  
Accepted 19<sup>th</sup> June 2014  
Published 5<sup>th</sup> August 2014

### ABSTRACT

Steady, laminar, incompressible and fully developed fluid flow of immiscible electrically conducting fluids between two infinite inclined parallel plates has been studied when the two plates are maintained at different constant temperatures  $T_{w1}$  and  $T_{w2}$ . A constant magnetic field  $B_0$  is applied transverse to the plates and a constant electric field  $E_0$  is applied across the channel. The whole system is rotated at an angular velocity about an axis perpendicular to the channel plates. The transport properties of the two fluids are taken to be constant. Approximate solutions for temperature, primary and secondary velocity distributions are obtained using regular perturbation method because the resulting equations are coupled and non-linear. It is observed that in the short circuit case ( $E = 0$ ), as rotation increases both the primary velocity and temperature distribution decrease where as secondary velocity oscillates. It is also observed that for the open circuit case ( $E = \pm 1$ ) as the rotation increases the secondary velocity becomes oscillatory. In case of  $E = -1$ , the increasing rotation tends to accelerate the primary velocity, but in case of positive  $E$ , it accelerates the primary velocity in the opposite direction. For the open circuit case ( $E = \pm 1$ ), as the rotation increases the temperature decreases for small values of rotation and increases for large rotation.

**Keywords:** Rotating fluids; heat transfer; magnetohydrodynamics; inclined channel; two-phase flow.

\*Corresponding author: Email: [drmurtypsr@gmail.com](mailto:drmurtypsr@gmail.com);

**Mathematics Subject Classification:** 76U05, 76TXX, 76W05, 76X05.

## NOMENCLATURE

$B_0$	:magnetic field strength
$b$	:ratio of the coefficients of thermal expansion, $(\beta_2/\beta_1)$
$C_p$	:specific heat at constant pressure
$E$	:Electric load parameter, $[E_0/(B_0 \bar{u}_1)]$
$E_0$	:Electric field strength
$Ec$	:Eckert number, $(\bar{u}_1)^2/(C_p \Delta T)$
$g$	:acceleration due to gravity
$h$	:ratio of the heights of the two phases, $(h_2/h_1)$
$Gr$	:Grashof number, $[g \beta_1 h_1^3 \Delta T / \nu_1^2]$
$K$	:ratio of the thermal conductivities, $(K_1/K_2)$
$K_1, K_2$	:thermal conductivities of phase I and II respectively
$M$	:Hartmann number, $B_0 h_1 \sqrt{(\sigma_1/\mu_1)}$
$m$	:ratio of the viscosities, $(\mu_1/\mu_2)$
$n$	:ratio of the densities $(\rho_2/\rho_1)$
$P$	:non dimensional pressure gradient, $[h_1^2(\partial p/\partial x)/\mu_1 \bar{u}_1]$
$Pr$	:Prandtl number, $(\mu_1 C_p / K_1)$
$Re$	:Reynolds number, $[(\bar{u}_1 h_1 / \nu_1)]$
$R$	:Rotation parameter, $[h_i \sqrt{\Omega / \nu}]$
$T$	:temperature
$T_{w1}, T_{w2}$	:temperature of the boundaries
$u$	:primary velocity
$w$	:secondary velocity
$\bar{u}_1$	:average velocity
$x, y, z$	:space coordinates

## Greek Symbols

$\beta$	:coefficient of thermal expansion
$\sigma$	:electrical conductivity
$\phi$	:angle of inclination
$\rho$	:density
$\nu$	:kinematic viscosity
$\mu$	:viscosity
$\varepsilon$	:product of Prandtl number and Eckert number ( $Pr \cdot Ec$ )
$\Delta T$	:difference in temperature $[T_{w1} - T_{w2}]$
$\theta$	:non dimensional temperature, $[(T - T_{w2})/\Delta T]$
$\Omega$	:angular velocity

## Subscript

$i$	:value for phase
-----	------------------

## 1. INTRODUCTION

The phenomenon of magnetohydrodynamic two-phase flow between two parallel plates with heat transfer aspects is of considerable importance in engineering and technology. In the chemical industry two-phase flows occur in both heat exchange equipment, gas-liquid contactors and chemical reactors such as packed column, spray and bubble columns, agitated vessels etc. Another important area where our knowledge of two-phase flow is vital is in nuclear reactor design (water-cooled reactors and sodium-cooled fast breeder reactors etc). Romig [1] studied the influence of electric and magnetic fields on heat transfer to electrically conducting fluids. Rudraiah et al. [2] analyzed nonlinear magnetoconvection and its applications to solar convection problems. Shail [3] studied the two-phase flow between two parallel insulated plates in which one phase being electrically conducting and the other phase is electrically non-conducting. Lohrasbi and Sahai [4] studied the MHD two-phase flow with heat transfer aspects in a horizontal channel in which one phase being electrically conducting and the other phase is electrically non-conducting. Malashetty and Leela [5] carried out a theoretical study on MHD heat transfer in two fluid flow for short circuit case. Subsequently, Malashetty and Leela [6] analyzed MHD heat transfer in two-phase flow by assuming that the fluid in both regions to be electrically conducting for the open circuit case. Raju and Murty [7] studied the hydromagnetic two-phase flow and heat transfer through two parallel plates in a rotating system for the open circuit case. Chauhan and Rastogi [8,9] discussed Hall current and heat transfer effects on MHD flow and MHD couette flow in a channel partially filled with a porous medium in a rotating system. Seth et al. [10] presented the Hartmann flow in a rotating system in the presence of inclined magnetic field with Hall effects. Recently, Raju and Valli [11] have studied the MHD two-layered unsteady flow and heat transfer through a horizontal channel in the presence of an applied magnetic and electric fields in a rotating system. In the present problem, hydromagnetic two fluid flow with heat transfer aspects between two infinite inclined parallel plates in a rotating frame of reference is investigated in the presence of a uniform electric field.

## 2. FORMULATION OF THE PROBLEM

The geometry under consideration consisting of a steady, laminar and fully developed two fluid magnetohydrodynamic convective flow driven by a constant pressure gradient  $(-\partial p/\partial x)$  between two infinite inclined parallel plates making an angle  $\phi$  with the horizontal. Fig. 1. illustrates the physical configuration. A magnetic field of uniform strength  $B_0$  is applied normal to the plates and the uniform electric field  $E_0$  is applied across the channel. The whole system is rotated with an angular velocity  $\Omega$  in a counter-clockwise direction about an axis normal to the plates. The regions  $0 \leq y \leq h_1$  and  $-h_2 \leq y \leq 0$  are occupied by two different electrically conducting incompressible fluids with different densities, viscosities, thermal and electrical conductivities. The transport properties of both fluids are taken to be constant.

With these assumptions, the governing equations of motion and energy for both phases are:

$$\mu_i \left( \frac{d^2 u_i}{dy^2} \right) + \rho_i g \beta_i (T_i - T_{w2}) \sin \phi - \sigma_i B_0 (E_0 + B_0 u_i) = \left( \frac{\partial p}{\partial x} \right) + 2\rho_i \Omega w_i \quad (1)$$

$$\mu_i \left( \frac{d^2 w_i}{dy^2} \right) - \sigma_i B_0^2 w_i = -2\rho_i \Omega u_i \tag{2}$$

$$\frac{d^2 T_i}{dy^2} + \frac{\mu_i}{K_i} \left[ \left( \frac{du_i}{dy} \right)^2 + \left( \frac{dw_i}{dy} \right)^2 \right] + \frac{\sigma_i}{K_i} \left[ E_0^2 + B_0^2 u_i^2 + B_0^2 w_i^2 + 2E_0 B_0 (u_i + w_i) \right] = 0 \tag{3}$$

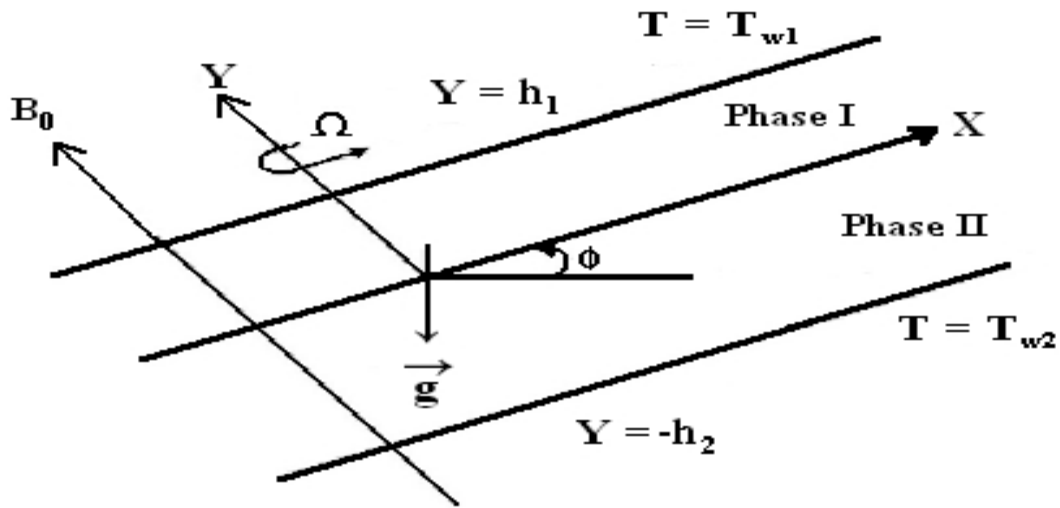


Fig. 1. Physical configuration

where  $u_i$  and  $w_i$  are the primary and secondary velocity components along x and z directions respectively,  $T_i$  is the temperature,  $\beta_i$  is the coefficient of thermal expansion,  $g$  is the acceleration due to gravity.

“By the addition of electromagnetic field, the fluid and the thermometric boundary conditions are unchanged. The no-slip condition demands the vanishing of velocity at the wall. In addition to the above conditions, the fluid velocity, shear stress, temperature and heat flux must be continuous across the interface”.

The boundary and interface conditions on primary and secondary velocity distributions are:

$$u_1(h_1) = 0, w_1(h_1) = 0; u_1(0) = u_2(0), w_1(0) = w_2(0); u_2(-h_2) = 0, w_2(-h_2) = 0; \tag{4}$$

$$\mu_1 \frac{du_1}{dy} = \mu_2 \frac{du_2}{dy} \text{ and } \mu_1 \frac{dw_1}{dy} = \mu_2 \frac{dw_2}{dy} \text{ at } y = 0 \tag{5}$$

Since the walls are maintained at constant different temperatures  $T_{w1}$  and  $T_{w2}$  at  $y = h_1$  and  $y = -h_2$  respectively, the boundary conditions on  $T_1$  and  $T_2$  are as follows:

$$T_1(h_1) = T_{w1}, \quad T_1(0) = T_2(0), \quad T_2(-h_2) = T_{w2}, \quad K_1 \frac{dT_1}{dy} = K_2 \frac{dT_2}{dy} \quad \text{at } y=0. \quad (6)$$

In making these equations dimensionless, the following transformations are used:

$$\begin{aligned} u_1^* &= \frac{u_1}{u_1}; & u_2^* &= \frac{u_2}{u_1}; & y_1^* &= \frac{y_1}{h_1}; & y_2^* &= \frac{y_2}{h_2}; & \theta &= \frac{(T - T_{w2})}{(T_{w1} - T_{w2})}; & m &= \frac{\mu_1}{\mu_2}; & E &= \frac{E_0}{B_0 u_1}; \\ K &= \frac{K_1}{K_2}; & h &= \frac{h_2}{h_1}; & n &= \frac{\rho_2}{\rho_1}; & b &= \frac{\beta_2}{\beta_1}; & Gr &= \frac{g \beta_1 h_1^3 (T_{w1} - T_{w2})}{\nu_1^2}; & Re &= \frac{\bar{u}_1 h_1}{\nu_1}; \\ M &= B_0 h_1 \sqrt{\frac{\sigma_1}{\mu_1}}; & Pr &= \frac{\mu_1 C_p}{K_1}; & P &= \left( \frac{h_1^2}{\mu_1 u_1} \right) \left( \frac{\partial p}{\partial x} \right); & Ec &= \frac{\bar{u}_1^2}{C_p (T_{w1} - T_{w2})}; & R^2 &= \frac{\Omega h_i^2}{\nu}. \end{aligned} \quad (7)$$

“Here Gr is the Grashof number, Ec is the Eckert number, Pr is the Prandtl number, Re is the Reynolds number, M is the Hartmann number, P is the non-dimensional pressure gradient and  $\bar{u}_1$  is the average velocity”. With the above non-dimensional quantities, the governing equations (1), (2) and (3) become:

$$\frac{d^2 u_i}{dy^2} + \frac{Gr}{Re} A \sin \phi \theta_i - B M^2 (E + u_i) = C P + 2R^2 w_i \quad (8)$$

$$\frac{d^2 w_i}{dy^2} - B M^2 w_i = -2R^2 u_i \quad (9)$$

$$\frac{d^2 \theta_i}{dy^2} + Pr Ec D \left[ \left( \frac{du_i}{dy} \right)^2 + \left( \frac{dw_i}{dy} \right)^2 \right] + Pr Ec F M^2 [E^2 + u_i^2 + w_i^2 + 2E(u_i + w_i)] = 0. \quad (10)$$

$$\text{Here } A = b m n h^2, \quad B = m s h^2, \quad C = m h^2, \quad D = K/m, \quad F = K h^2 s \quad (11)$$

and A, B, C, D and F are all equal to 1 for phase-I.

The non-dimensional forms of the boundary and interface conditions from (4) to (6) will transform as:

$$u_1(1) = 0; \quad w_1(1) = 0; \quad u_1(0) = u_2(0); \quad w_1(0) = w_2(0); \quad u_2(-1) = 0; \quad w_2(-1) = 0; \quad (12)$$

$$\frac{du_1}{dy} = \frac{1}{mh} \frac{du_2}{dy} \quad \text{and} \quad \frac{dw_1}{dy} = \frac{1}{mh} \frac{dw_2}{dy} \quad \text{at } y=0. \quad (13)$$

$$\theta_1(1) = 1, \theta_1(0) = \theta_2(0), \theta_2(-1) = 0, \frac{d\theta_1}{dy} = \frac{1}{Kh} \frac{d\theta_2}{dy} \text{ at } y = 0 \quad (14)$$

The asterisks have been dropped for simplicity.

$$\text{Further writing } q_1 = u_1 + iw_1 \text{ and } q_2 = u_2 + iw_2, \quad (15)$$

equations (8), (9) and (10) can be written in complex form as:

$$\left(\frac{d^2 q_i}{dy^2}\right) + \left(\frac{Gr}{Re}\right) A \sin \phi \theta_i - B M^2 q_i = C P + B M^2 E - 2 i R^2 q_i \quad (16)$$

$$\left(\frac{d^2 \theta_i}{dy^2}\right) + Pr Ec D \left[ \left(\frac{dq_i}{dy}\right) \left(\frac{d\bar{q}_i}{dy}\right) \right] + Pr Ec F M^2 \left[ E^2 + (q_i \bar{q}_i) + E(q_i + \bar{q}_i) - i E(q_i - \bar{q}_i) \right] = 0 \quad (17)$$

which are to be solved subject to the boundary and interface conditions:

$$q_1(1) = 0, q_1(0) = q_2(0), q_2(-1) = 0, \frac{dq_1}{dy} = \frac{1}{mh} \frac{dq_2}{dy} \text{ at } y = 0 \quad (18)$$

$$\theta_1(1) = 1, \theta_1(0) = \theta_2(0), \theta_2(-1) = 0, \frac{d\theta_1}{dy} = \frac{1}{Kh} \frac{d\theta_2}{dy} \text{ at } y = 0 \quad (19)$$

### 3. SOLUTIONS

The governing equations of motion (16) and energy (17) are to be solved subject to the boundary and interface conditions (18) and (19). Due to the inclusion of the dissipation terms, the equations are coupled and non-linear and the solutions of which are obtained using perturbation technique. Since the Eckert number is of order  $10^{-5}$  and is very small, the product  $Pr Ec (= \epsilon)$  is very small and is used in the regular perturbation method. The solutions are assumed in the following form:

$$(q_i, \theta_i) = (q_{i0}, \theta_{i0}) + \epsilon(q_{i1}, \theta_{i1}) + \dots \quad (20)$$

where  $q_{i0}, \theta_{i0}$  are solutions for the case  $\epsilon$  equal to zero.  $q_{i1}, \theta_{i1}$  are perturbed quantities relating to  $q_{i0}, \theta_{i0}$  respectively. Substituting the above solutions in the equations (16), (17) and then equating the coefficients of like powers of  $\epsilon$  to zero, we get the zeroth and first order equations as follows:

### 3.1 Zeroth Order Equations

$$\frac{d^2 q_{i0}}{dy^2} + \frac{Gr}{Re} A \sin \phi \theta_{i0} - B M^2 q_{i0} = CP + B M^2 E - 2i R^2 q_{i0} \quad (21)$$

$$\frac{d^2 \theta_{i0}}{dy^2} = 0 \quad (22)$$

### 3.2 First Order Equations

$$\frac{d^2 q_{i1}}{dy^2} + \frac{Gr}{Re} A \sin \phi \theta_{i1} - B M^2 q_{i1} = -2i R^2 q_{i1} \quad (23)$$

$$\frac{d^2 \theta_{i1}}{dy^2} + D \left[ \frac{dq_{i0}}{dy} \frac{d\bar{q}_{i0}}{dy} \right] + F M^2 \left[ E^2 + (q_{i0} \bar{q}_{i0}) + E(q_{i0} + \bar{q}_{i0}) - i E(q_{i0} - \bar{q}_{i0}) \right] = 0. \quad (24)$$

The corresponding boundary conditions (18) and (19) reduce to:

$$q_{10}(1) = 0, q_{10}(0) = q_{20}(0), q_{20}(-1) = 0, \frac{dq_{10}}{dy} = \frac{1}{mh} \frac{dq_{20}}{dy} \text{ at } y = 0 \quad (25)$$

$$\theta_{10}(1) = 1, \theta_{10}(0) = \theta_{20}(0), \theta_{20}(-1) = 0, \frac{d\theta_{10}}{dy} = \frac{1}{Kh} \frac{d\theta_{20}}{dy} \text{ at } y = 0 \quad (26)$$

$$q_{11}(1) = 0, q_{11}(0) = q_{21}(0), q_{21}(-1) = 0, \frac{dq_{11}}{dy} = \frac{1}{mh} \frac{dq_{21}}{dy} \text{ at } y = 0 \quad (27)$$

$$\theta_{11}(1) = 0, \theta_{11}(0) = \theta_{21}(0), \theta_{21}(-1) = 0, \frac{d\theta_{11}}{dy} = \frac{1}{Kh} \frac{d\theta_{21}}{dy} \text{ at } y = 0. \quad (28)$$

We note that  $q_{10} = u_{10} + iw_{10}$ ,  $q_{20} = u_{20} + iw_{20}$ ,  $q_{11} = u_{11} + iw_{11}$  and  $q_{21} = u_{21} + iw_{21}$ . (29)

Solutions of the zeroth order equations (21) and (22) using boundary conditions (25) and (26) are as follows:

$$\theta_{10} = \frac{y + Kh}{1 + Kh} \quad (30)$$

$$\theta_{20} = \frac{K h(1+y)}{1+K h} \tag{31}$$

$$u_{10} = (c_{13} e^{d_6 y} + c_{14} e^{-d_6 y}) \cos d_7 y + d_{13} y + d_{15} \tag{32}$$

$$w_{10} = -\left( (c_{13} e^{d_6 y} - c_{14} e^{-d_6 y}) \sin d_7 y - d_{14} y - d_{16} \right) \tag{33}$$

$$u_{20} = (c_{15} e^{d_{23} y} + c_{16} e^{-d_{23} y}) \cos d_{24} y + d_{30} + d_{32} y \tag{34}$$

$$w_{20} = -\left( (c_{15} e^{d_{23} y} - c_{16} e^{-d_{23} y}) \sin d_{24} y - d_{31} - d_{33} y \right) \tag{35}$$

Solutions of the first order equations (23) and (24) using boundary conditions (27) and (28) are:

$$\begin{aligned} \theta_{11} = & \{c_{17} y + c_{18} + d_{136} e^{2d_6 y} + d_{137} \cos 2d_7 y + d_{138} e^{-2d_6 y} + d_{212} e^{d_6 y} \sin d_7 y \\ & + d_{213} e^{d_6 y} \cos d_7 y + d_{214} e^{-d_6 y} \sin d_7 y + d_{215} e^{-d_6 y} \cos d_7 y \\ & + d_{216} e^{d_6 y} y \cos d_7 y + d_{217} e^{d_6 y} y \sin d_7 y + d_{218} e^{-d_6 y} y \cos d_7 y \\ & + d_{219} e^{-d_6 y} y \sin d_7 y + d_{176} y^4 + d_{177} y^3 + d_{178} y^2\} + i\{d_{179} \sin 2d_7 y \\ & + d_{220} e^{d_6 y} \sin d_7 y + d_{221} e^{d_6 y} \cos d_7 y + d_{222} e^{-d_6 y} \sin d_7 y \\ & + d_{223} e^{-d_6 y} \cos d_7 y + d_{224} e^{d_6 y} y \cos d_7 y + d_{225} e^{d_6 y} y \sin d_7 y \\ & + d_{226} e^{-d_6 y} y \cos d_7 y + d_{999} e^{-d_6 y} y \sin d_7 y \end{aligned} \tag{36}$$

$$\begin{aligned} \theta_{21} = & \{c_{19} y + c_{20} + d_{371} e^{2d_{23} y} + d_{304} \cos 2d_{24} y + d_{305} e^{-2d_{23} y} + d_{372} e^{d_{23} y} \sin d_{24} y \\ & + d_{373} e^{d_{23} y} \cos d_{24} y + d_{374} e^{-d_{23} y} \sin d_{24} y + d_{375} e^{-d_{23} y} \cos d_{24} y \\ & + d_{376} e^{d_{23} y} y \cos d_{24} y + d_{377} e^{d_{23} y} y \sin d_{24} y + d_{378} e^{-d_{23} y} y \cos d_{24} y \\ & + d_{379} e^{-d_{23} y} y \sin d_{24} y - d_{343} y^4 - d_{344} y^3 - d_{345} y^2\} + i\{d_{346} \sin 2d_{24} y \\ & + d_{380} e^{d_{23} y} \sin d_{24} y + d_{381} e^{d_{23} y} \cos d_{24} y + d_{382} e^{-d_{23} y} \sin d_{24} y \\ & + d_{383} e^{-d_{23} y} \cos d_{24} y + d_{384} e^{d_{23} y} y \cos d_{24} y + d_{385} e^{d_{23} y} y \sin d_{24} y \\ & + d_{386} e^{-d_{23} y} y \cos d_{24} y + d_{387} e^{-d_{23} y} y \sin d_{24} y\} \end{aligned} \tag{37}$$



$$\begin{aligned}
 u_{11} = & \left( c_{21} e^{d_6 y} + c_{22} e^{-d_6 y} \right) \cos d_7 y + g_{95} e^{2d_6 y} + g_{96} e^{-2d_6 y} - g_{97} \cos 2d_7 y \\
 & + g_{98} \sin 2d_7 y + g_{99} e^{d_6 y} y \sin d_7 y + g_{100} e^{d_6 y} y \cos d_7 y + g_{101} e^{-d_6 y} y \cos d_7 y \\
 & + g_{102} e^{-d_6 y} y \sin d_7 y + g_{103} e^{d_6 y} y^2 \sin d_7 y + g_{104} e^{d_6 y} y^2 \cos d_7 y \\
 & + g_{105} e^{-d_6 y} y^2 \sin d_7 y + g_{106} e^{-d_6 y} y^2 \cos d_7 y - g_{107} y^4 - g_{108} y^3 + g_{109} y^2 \\
 & + g_{110} y + g_{111}
 \end{aligned} \tag{38}$$

$$\begin{aligned}
 w_{11} = & \left( c_{22} e^{-d_6 y} - c_{21} e^{d_6 y} \right) \sin d_7 y - g_{112} e^{2d_6 y} - g_{113} e^{-2d_6 y} \\
 & - g_{114} \cos 2d_7 y - g_{115} \sin 2d_7 y + g_{116} e^{d_6 y} y \cos d_7 y + g_{117} e^{d_6 y} y \sin d_7 y \\
 & + g_{118} e^{-d_6 y} y \sin d_7 y + g_{119} e^{-d_6 y} y \cos d_7 y + g_{120} e^{d_6 y} y^2 \sin d_7 y \\
 & + g_{121} e^{d_6 y} y^2 \cos d_7 y + g_{122} e^{-d_6 y} y^2 \sin d_7 y + g_{123} e^{-d_6 y} y^2 \cos d_7 y \\
 & - g_{124} y^4 - g_{125} y^3 + g_{126} y^2 + g_{127} y + g_{128}
 \end{aligned} \tag{39}$$

$$\begin{aligned}
 u_{21} = & \left( c_{23} e^{d_{23} y} + c_{24} e^{-d_{23} y} \right) \cos d_{24} y + g_{225} e^{2d_{23} y} + g_{226} e^{-2d_{23} y} + g_{227} \cos 2d_{24} y \\
 & - g_{228} \sin 2d_{24} y + g_{229} e^{d_{23} y} y \sin d_{24} y + g_{230} e^{d_{23} y} y \cos d_{24} y \\
 & + g_{231} e^{-d_{23} y} y \cos d_{24} y + g_{232} e^{-d_{23} y} y \sin d_{24} y + g_{233} e^{d_{23} y} y^2 \sin d_{24} y \\
 & + g_{234} e^{d_{23} y} y^2 \cos d_{24} y + g_{235} e^{-d_{23} y} y^2 \sin d_{24} y + g_{236} e^{-d_{23} y} y^2 \cos d_{24} y \\
 & + g_{237} y^4 + g_{238} y^3 + g_{239} y^2 + g_{240} y + g_{241}
 \end{aligned} \tag{40}$$

$$\begin{aligned}
 w_{21} = & \left( c_{24} e^{-d_{23} y} - c_{23} e^{d_{23} y} \right) \sin d_{24} y - g_{242} e^{2d_{23} y} - g_{243} e^{-2d_{23} y} \\
 & + g_{244} \cos 2d_{24} y + g_{245} \sin 2d_{24} y + g_{246} e^{d_{23} y} y \sin d_{24} y + g_{247} e^{d_{23} y} y \cos d_{24} y \\
 & + g_{248} e^{-d_{23} y} y \cos d_{24} y + g_{249} e^{-d_{23} y} y \sin d_{24} y + g_{250} e^{d_{23} y} y^2 \sin d_{24} y \\
 & + g_{251} e^{d_{23} y} y^2 \cos d_{24} y + g_{252} e^{-d_{23} y} y^2 \sin d_{24} y + g_{253} e^{-d_{23} y} y^2 \cos d_{24} y \\
 & + g_{254} y^4 + g_{255} y^3 + g_{256} y^2 + g_{257} y + g_{258}
 \end{aligned} \tag{41}$$

The constants involved in equations from (32) to (41) are not given for the sake of brevity. Solutions of zeroth and first order equations from (21) to (24) are solved numerically, fixing some of the parameters namely  $P=-5$ ,  $b=1$ ,  $Re=5$ ,  $n=1.5$  and  $K=1$ . The varying parameters are  $M$ ,  $Gr$ ,  $\Phi$ ,  $m$ ,  $h$ ,  $s$  and  $R$ . As the zeroth order solutions are linear, only first order temperature profiles are drawn. This shows that the heat transfer up to the zeroth order is only due to the conduction. In the figures., all the other parameters except the varying one are chosen from the set  $(M, Gr, \phi, m, h, s, R) = (2, 5, 30^\circ, 0.5, 1, 2, 2)$ .

#### 4. CONCLUSIONS

Magnetohydrodynamic two fluid flow with heat transfer aspects in an inclined channel is studied analytically. The resulting differential equations are solved using regular perturbation method for obtaining approximate solutions for temperature, primary and secondary velocity distributions.

The effect of rotation parameter  $R$  and the electric load parameter  $E$  on primary and secondary velocity distributions is discussed in the two cases  $E=0$  and  $E=\pm 1$ . The short circuit case ( $E=0$ ) for both the velocities is considered in the Figs. 2 and 3. The open circuit case ( $E=\pm 1$ ) for primary velocity is considered in Figs. 4, 5 and the same case for secondary velocity is shown in Figs. 6 and 7. It is observed that for  $E=0$  the effect of increasing rotation parameter is to decrease the primary velocity distribution. But for  $E=0$ , as the rotation increases the secondary velocity oscillates. In the case  $E=-1$  the increasing rotation tends to accelerate the primary velocity but in case of positive  $E$ , it accelerates the primary velocity in the opposite direction. In the open circuit case ( $E=\pm 1$ ), as the rotation increases the secondary velocity becomes oscillatory. Figs. 8 and 9 represent the effect of electric load parameter  $E$  and the ratio of viscosities  $m$  on primary and secondary velocity distributions respectively. In the case  $E=1$ , both primary and secondary velocities decrease for increasing values of  $m$  where as in case of negative  $E$ , both the velocities increase as  $m$  increases. The effect of electric load parameter  $E$  and the Hartmann number  $M$  on primary and secondary velocities is shown in Figs. 10 and 11 respectively. In case of negative  $E$ , as  $M$  increases, primary velocity increases but secondary velocity decreases. In the case  $E=1$ , as  $M$  increases primary velocity decreases and secondary velocity oscillates.

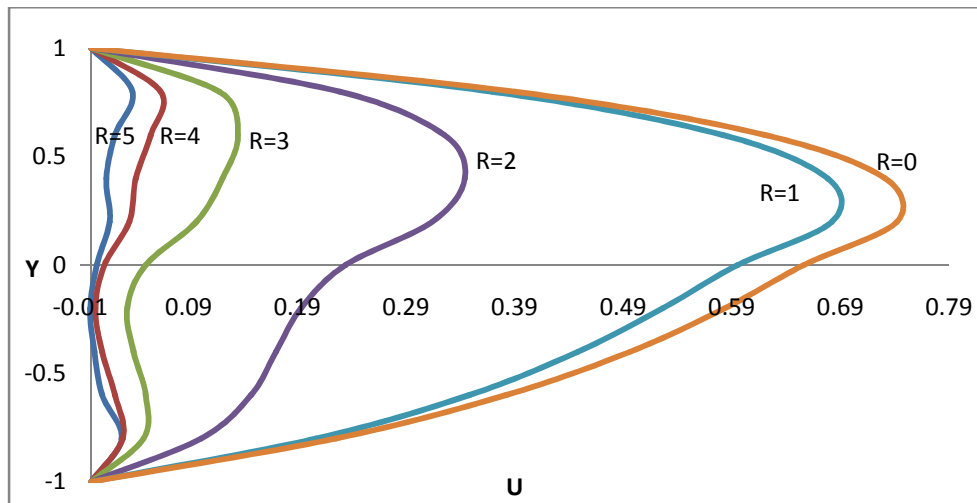


Fig. 2. Primary velocity profiles for different values of rotation parameter  $R$  for  $E=0$

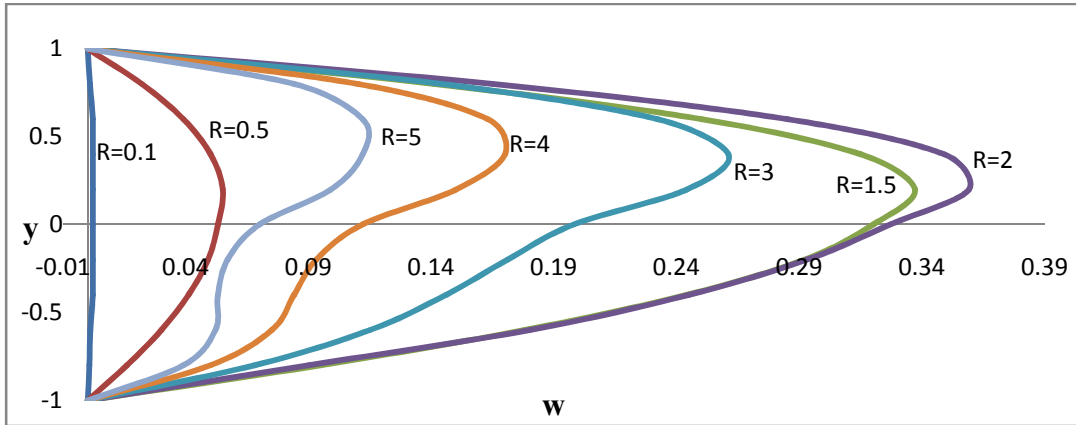


Fig. 3. Secondary velocity profiles for different values of rotation parameter R for E=0

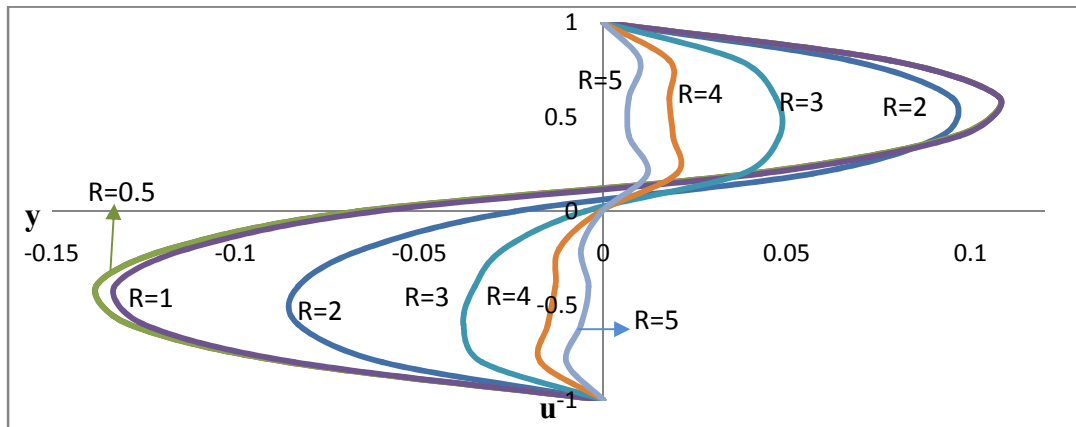


Fig. 4. Primary velocity profiles for different values of rotation parameter R for E=1

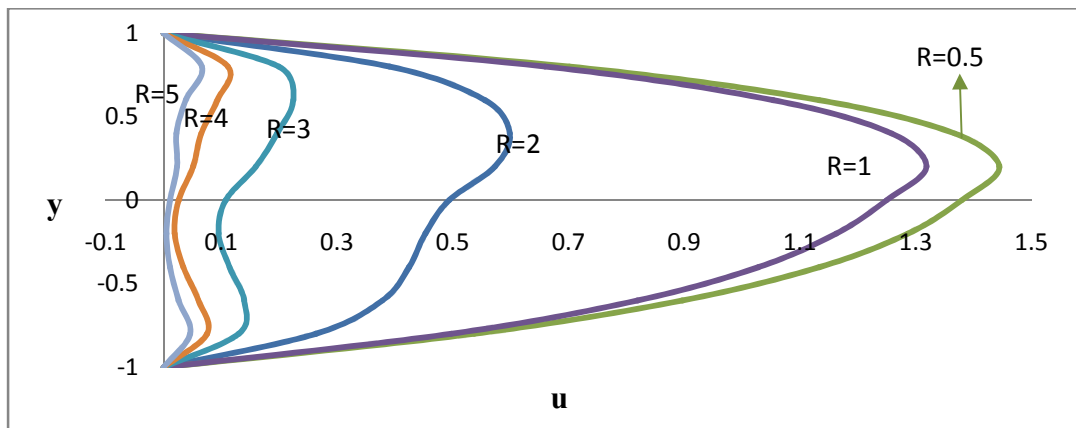


Fig. 5. Primary velocity profiles for different values of rotation parameter R for E=-1

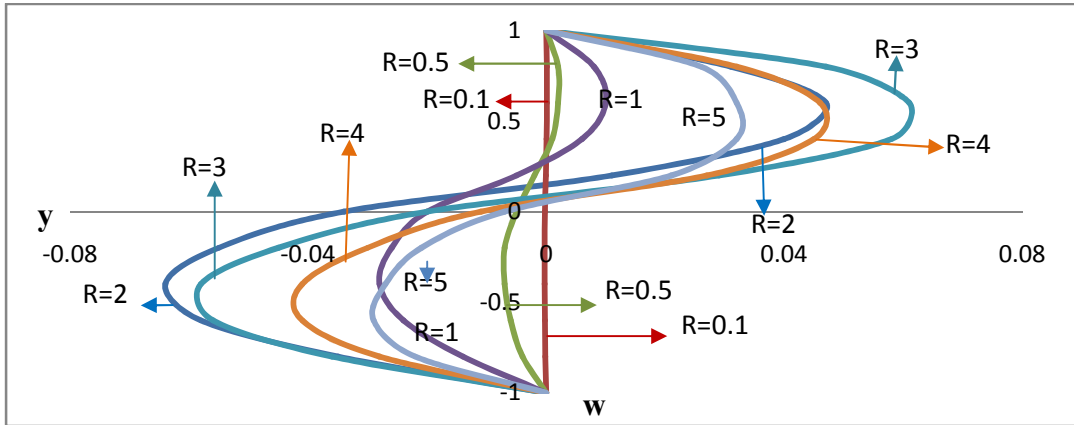


Fig. 6. Secondary velocity profiles for different values of rotation parameter  $R$  for  $E = 1$

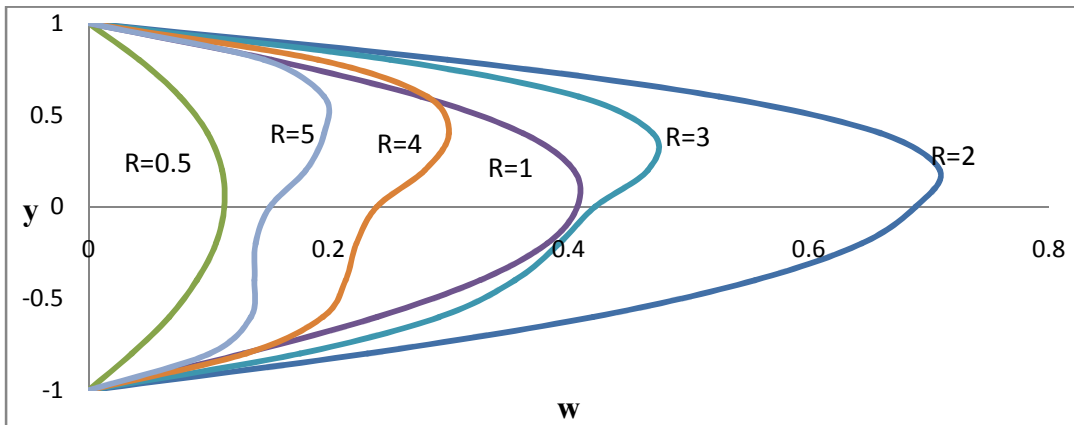


Fig. 7. Secondary velocity profiles for different values of Rotation parameter  $R$  for  $E = -1$

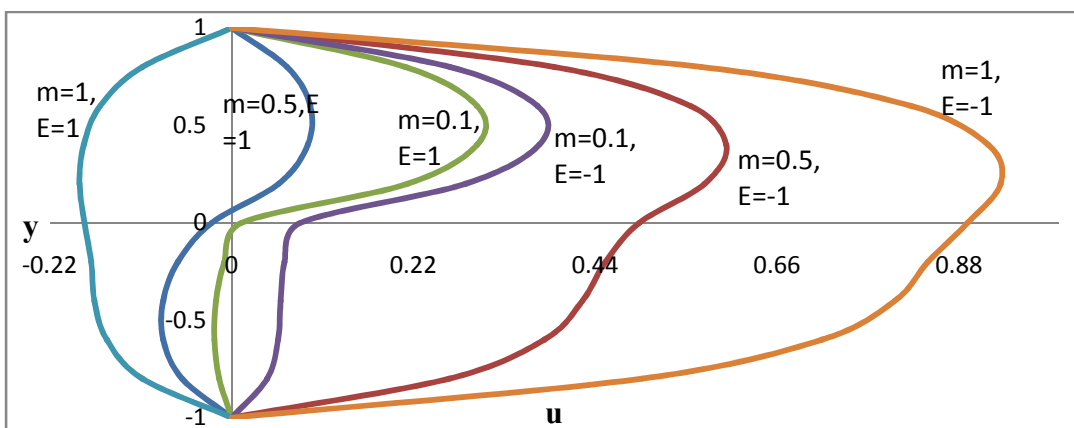


Fig. 8. Primary velocity profiles for different values of ratio of viscosities  $m$  for  $E = \pm 1$

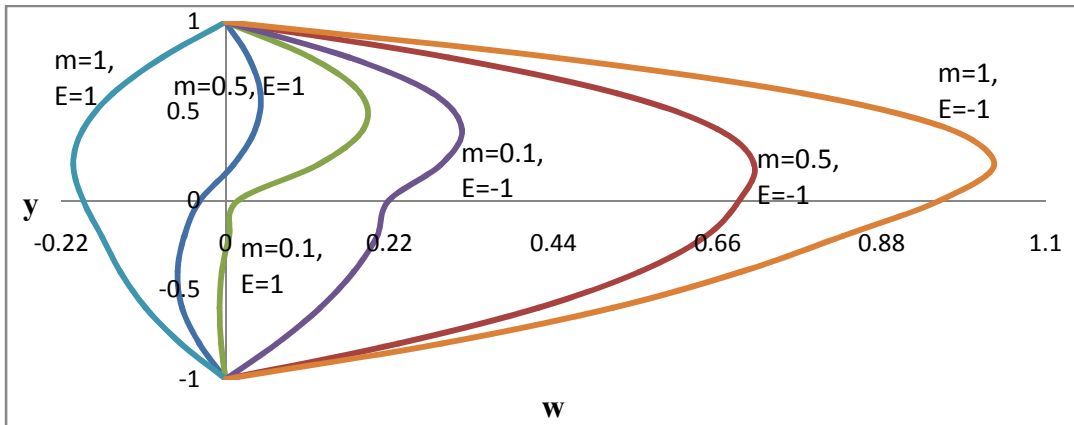


Fig. 9. Secondary velocity profiles for different values of ratio of viscosities  $m$  for  $E = \pm 1$

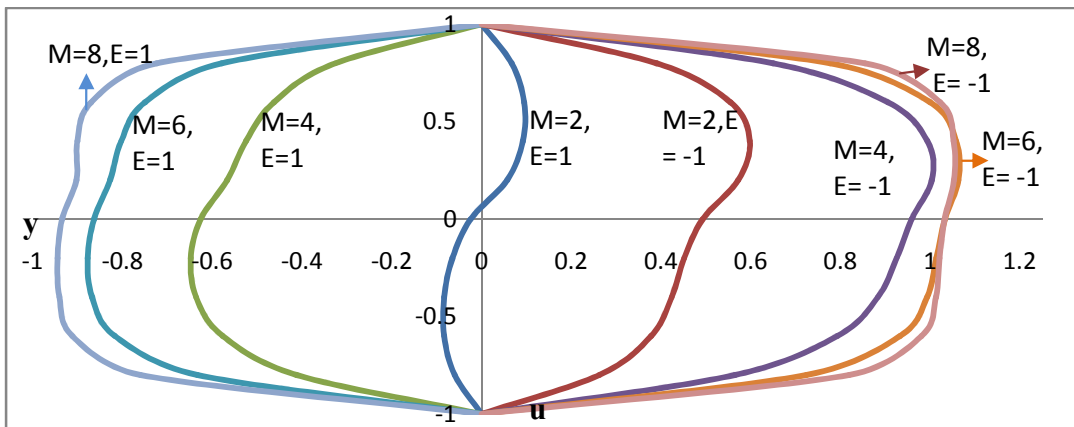


Fig. 10. Primary velocity profiles for different values of Hartmann number  $M$  for  $E = \pm 1$

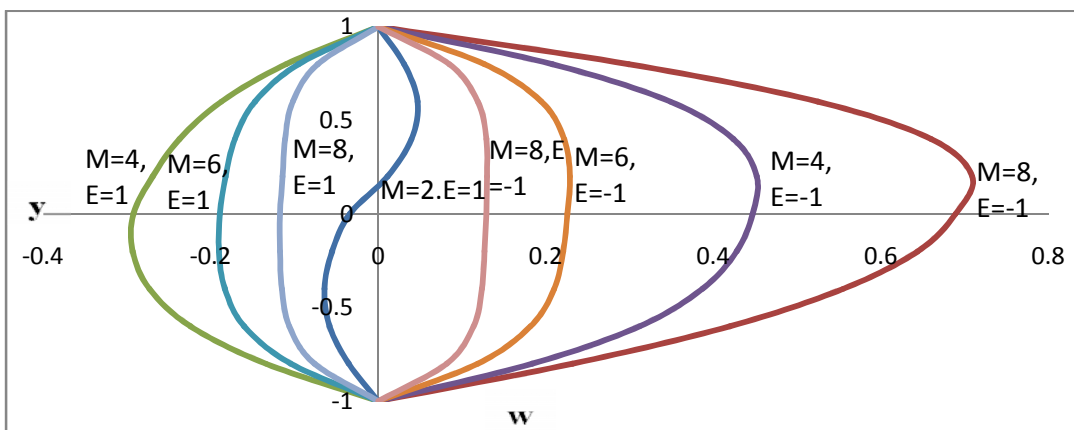


Fig. 11. Secondary velocity profiles for different values of Hartman number  $M$  for  $E = \pm 1$

Figs. 12 and 13 show the effect of  $E$  and the inclination angle  $\Phi$  on primary and secondary velocities respectively. From the figures, it is observed that in the open circuit case ( $E=\pm 1$ ) both the velocities increase for increasing values of  $\Phi$ . The effect of  $E$  and Grashof number  $Gr$ , on primary and secondary velocities is shown in Figs. 14 and 15 respectively. As the Grashof number  $Gr$  increases, both the velocities also increase. Figs. 16 and 17 represent the effect of  $E$  and the ratio of heights  $h$  on primary and secondary velocities respectively. It is concluded that for increasing values of  $h$ , both the velocities increase in case of  $E = -1$  and decrease in case of  $E = 1$ . The effect of  $E$  and the ratio of electrical conductivities  $s$  on primary and secondary velocities is represented in Figs. 18 and 19 respectively. From the figures, it is observed that as  $s$  increases, both the velocities also increase in case of  $E=-1$  and decrease in case of  $E=1$ . The effect of electric load parameter  $E$  and the rotation parameter  $R$  on temperature distribution  $\theta$  in the three cases  $E=0$ ,  $E=+1$  and  $E=-1$  is shown in Figs. 20, 21 and 22 respectively. It is observed that for the short circuit case ( $E=0$ ), as the rotation increases, the temperature decreases. While for the open circuit case ( $E=\pm 1$ ), as the rotation increases, the temperature decreases for small values of rotation and increases for large rotation (say  $R=2, 5$  etc). Fig. 23 shows the effect of  $E$  and the ratio of viscosities  $m$  on the temperature distribution. In the open circuit case ( $E=\pm 1$ ), the temperature distribution decreases for increasing values of  $m$ . The effect of  $E$  and the Hartmann number  $M$  on the temperature distribution is represented in Fig. 24. From the figure, it is noticed that as the Hartmann number  $M$  increases, the temperature distribution decreases. Fig. 25 represents the effect of the inclination angle  $\Phi$  and electric load parameter  $E$  on temperature distribution. We observe that as the inclination angle  $\Phi$  increases, the temperature increases in case of  $E=1$  and decreases in case of  $E=-1$ . The effect of  $E$  and the ratio of heights  $h$  on the temperature distribution is shown in Fig. 26. From the figure, it is identified that for the increasing values of  $h$ , the temperature also increases in case of  $E=1$  but in case of  $E=-1$ , the temperature increases for small values of  $h$  and decreases for large values of  $h$ . The effect of electric load parameter  $E$  and the Grashof number  $Gr$  on temperature distribution is represented in Fig. 27. It is observed that in case of positive  $E$ , the increasing Grashof number tends to accelerate the temperature, but in case of negative  $E$ , it accelerates the temperature in the opposite direction.

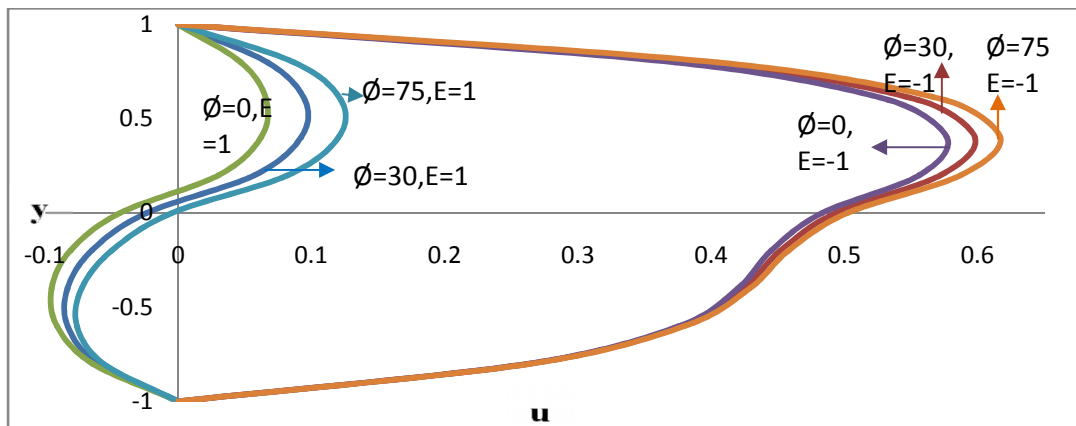


Fig. 12. Primary velocity profiles for different values of angle of inclination  $\Phi$  for  $E = \pm 1$

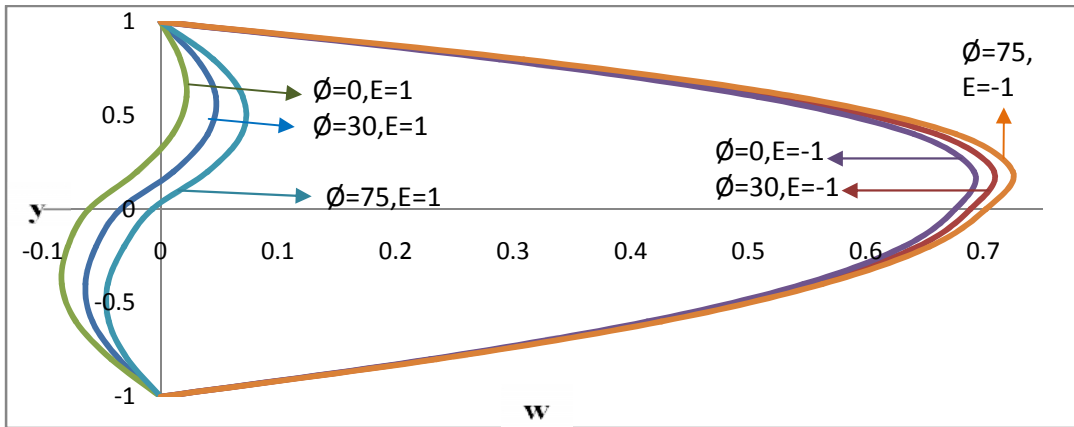


Fig. 13. Secondary velocity profiles for different values of angle of inclination  $\phi$  for  $E = \pm 1$

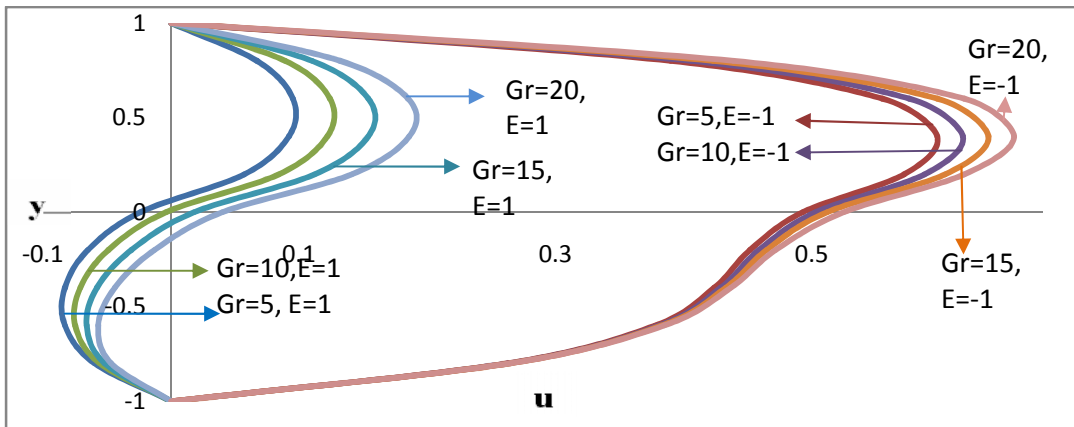


Fig. 14. Primary velocity profiles for different values of Grashof number  $Gr$  for  $E = \pm 1$

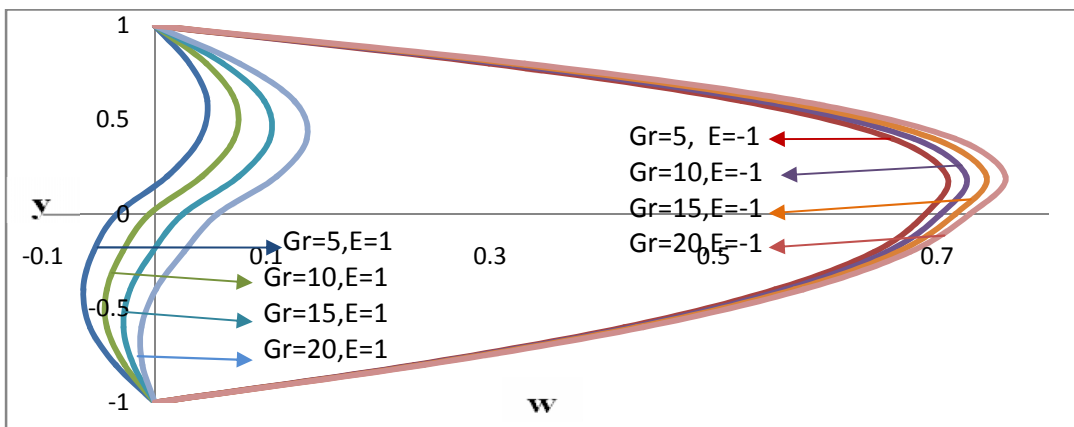


Fig. 15. Secondary velocity profiles for different values of Grashof number  $Gr$  for  $E = \pm 1$

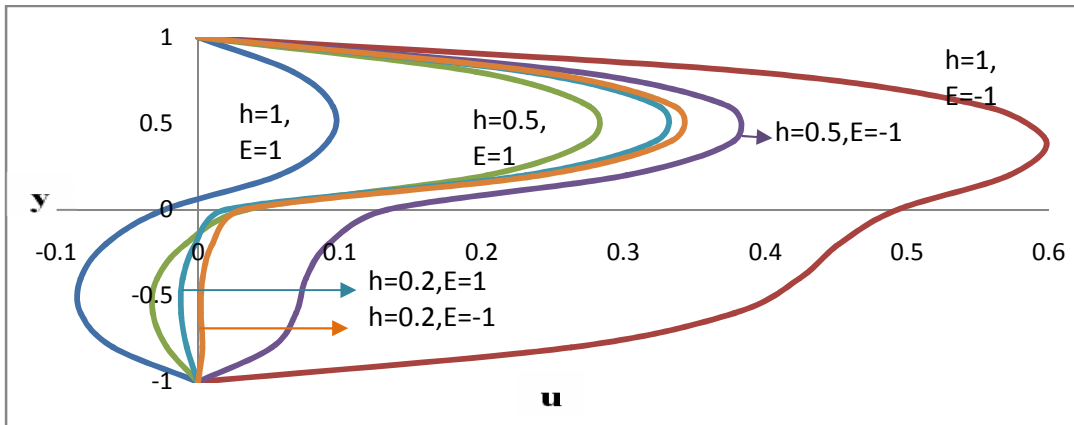


Fig. 16. Primary velocity profiles for different values of ratio of heights  $h$  for  $E = \pm 1$

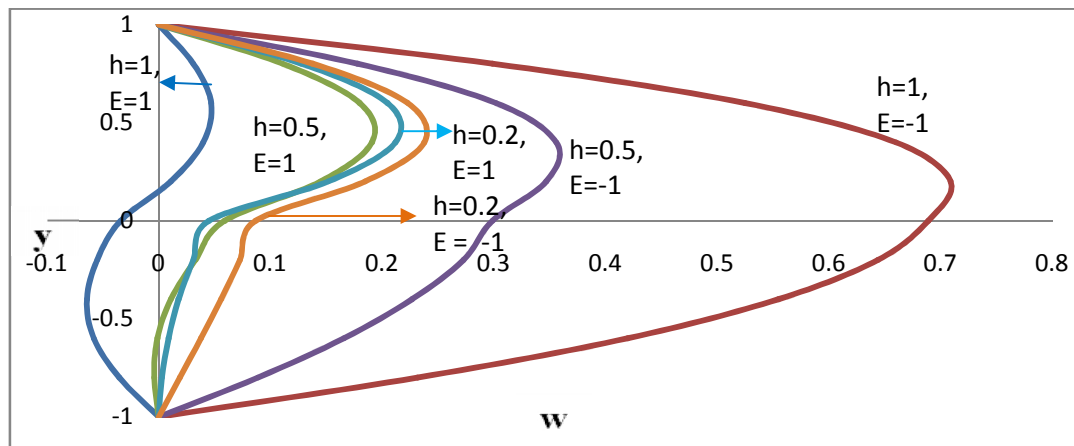


Fig. 17. Secondary velocity profiles for different values of ratio of heights  $h$  for  $E = \pm 1$

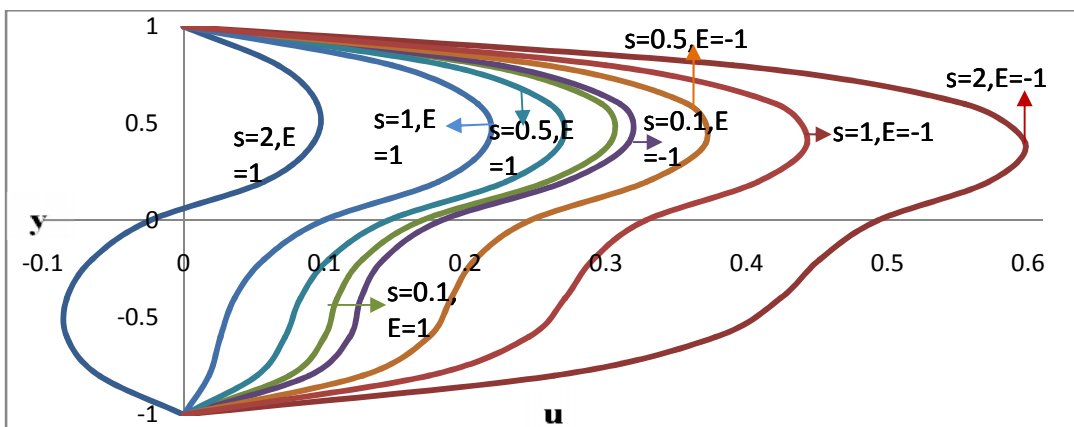


Fig. 18. Primary velocity profiles for different values of  $s$  for  $E = \pm 1$



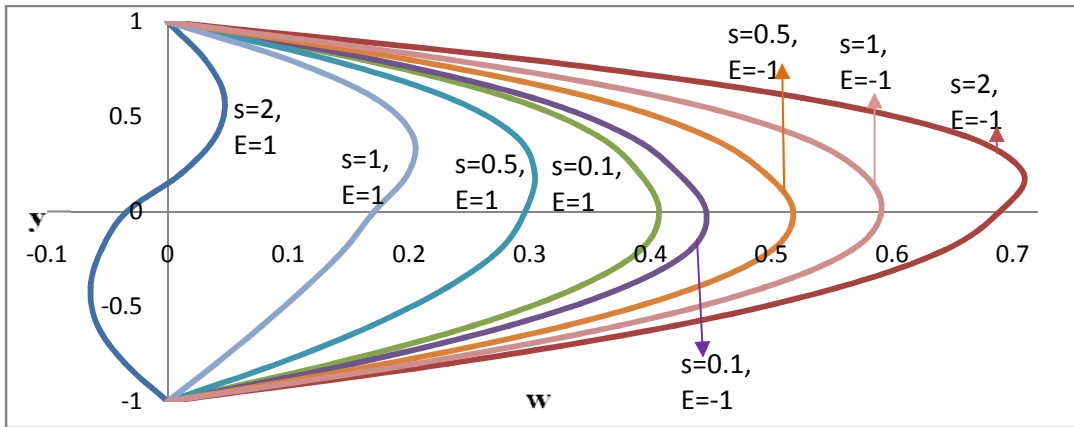


Fig. 19. Secondary velocity profiles for different values of  $s$  for  $E = \pm 1$

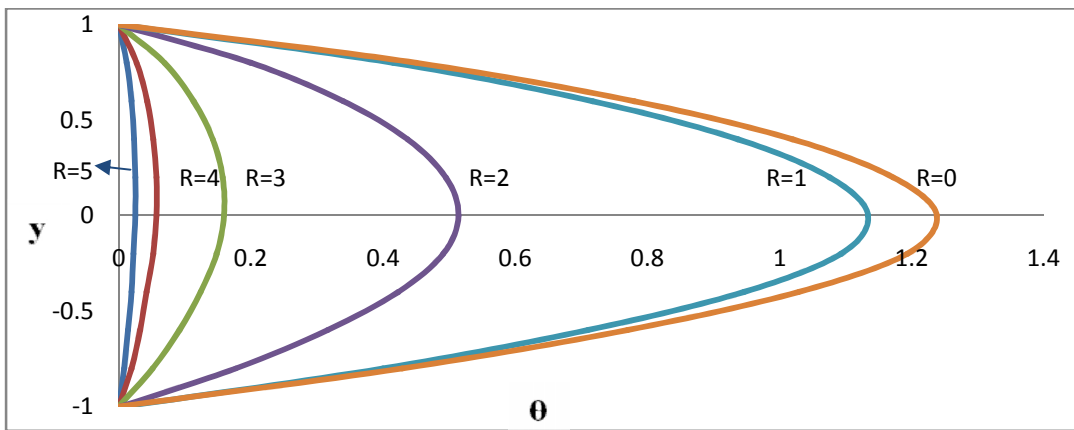


Fig. 20. Temperature profiles for different values of Rotation parameter  $R$  for  $E=0$

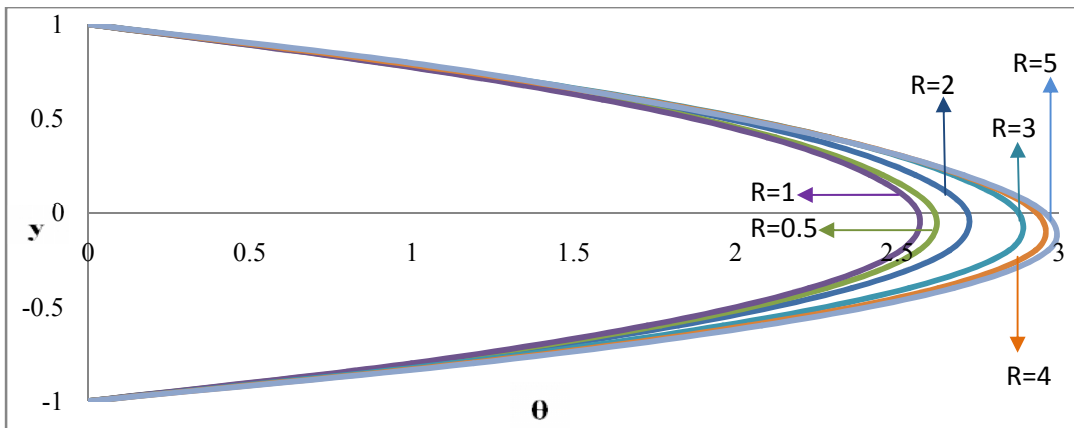


Fig. 21. Temperature profiles for different values of Rotation parameter  $R$  for  $E = 1$

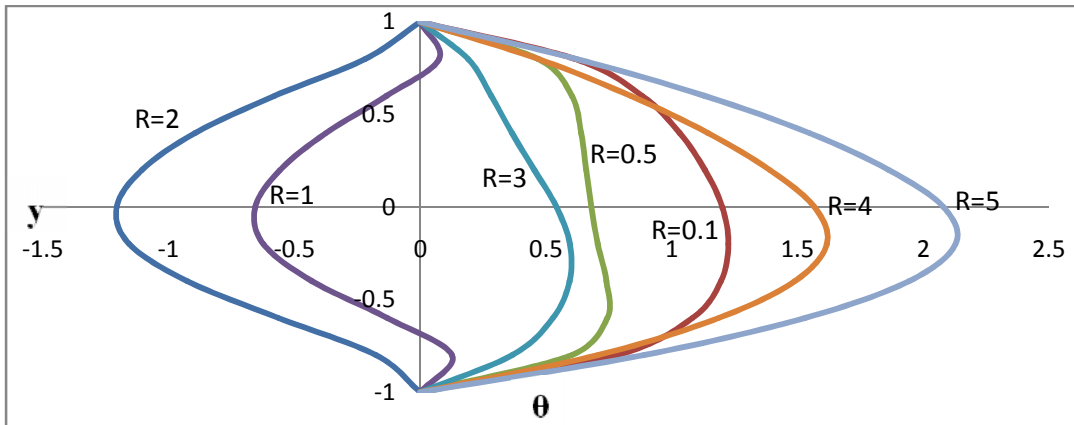


Fig. 22. Temperature profiles for different values of Rotation parameter  $R$  for  $E = -1$

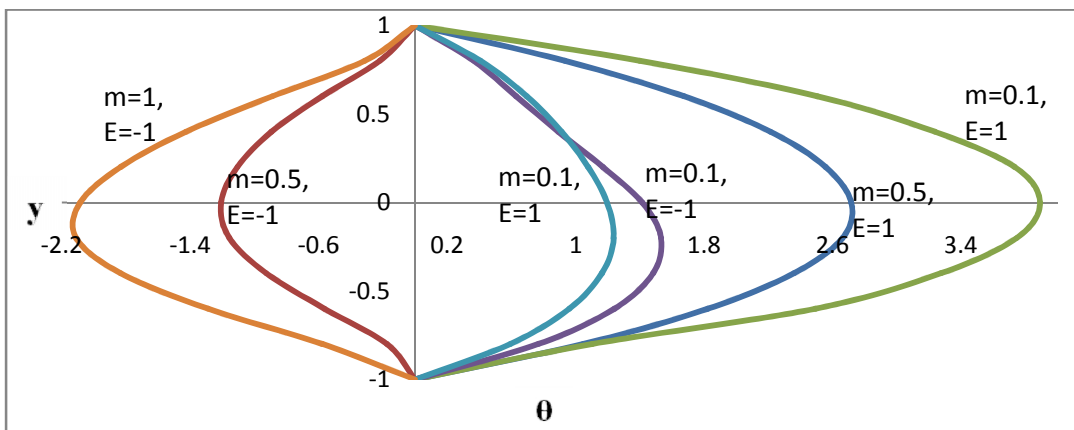


Fig. 23. Temperature profiles for different values of ratio of viscosities  $m$  for  $E = \pm 1$

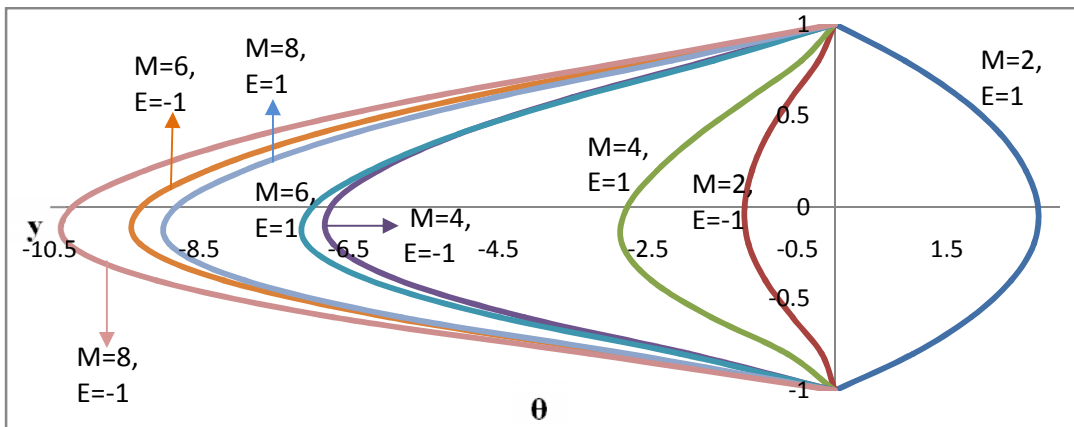


Fig. 24. Temperature profiles for different values of Hartman number  $M$  for  $E = \pm 1$

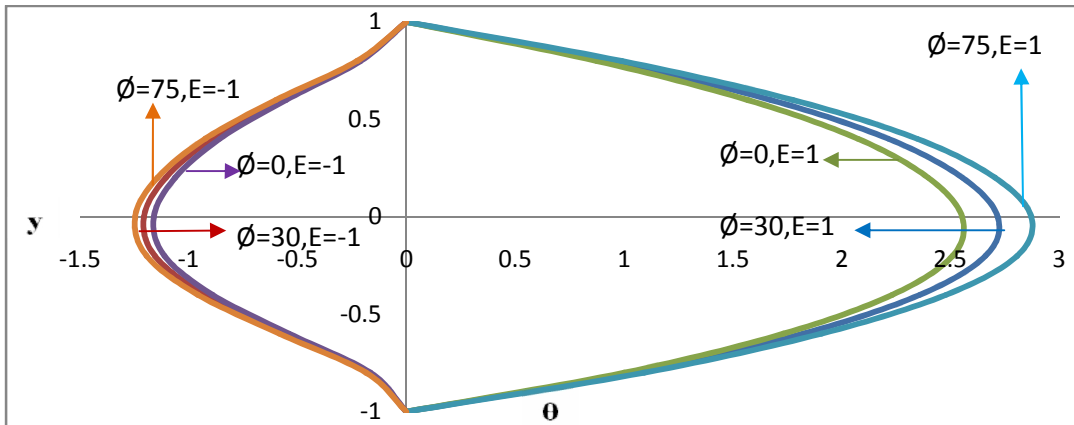


Fig. 25. Temperature profiles for different values of angle of inclination  $\varnothing$  for  $E = \pm 1$

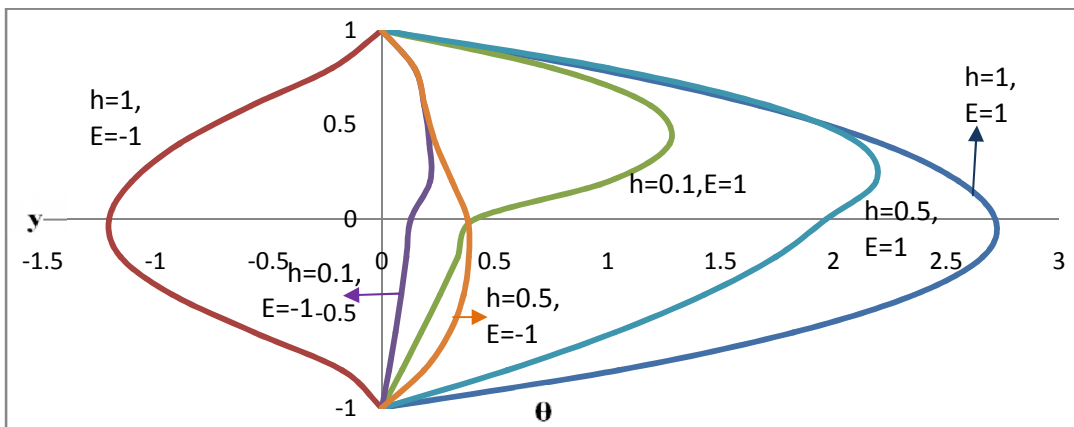


Fig. 26. Temperature profiles for different values of ratio of heights  $h$  for  $E = \pm 1$

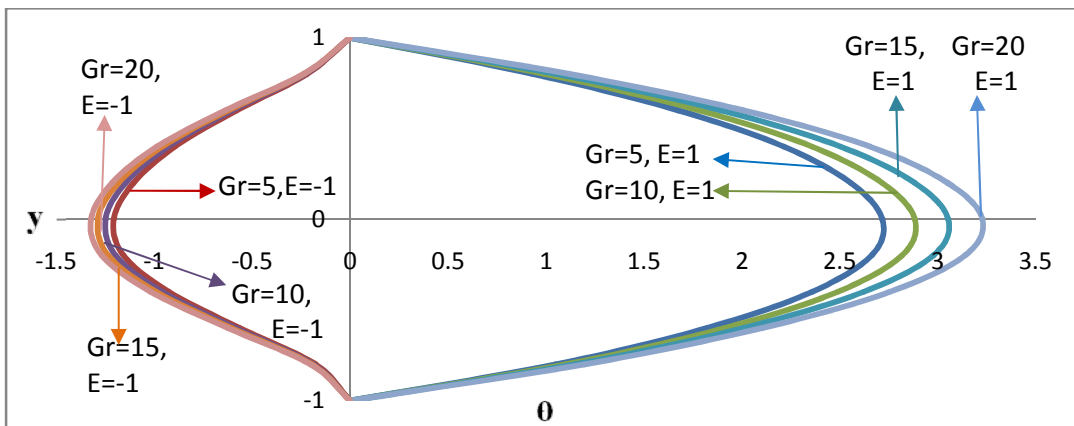


Fig. 27. Temperature profiles for different values of Grashof number  $Gr$  for  $E = \pm 1$

## COMPETING INTERESTS

Authors have declared that no competing interests exist.

## REFERENCES

1. Romig MF. The influence of electric and magnetic fields on heat transfer to electrically conducting fluids. Adv. Heat Transfer, Academic Press, New York. 1961;1.
2. Rudraiah N, Kumudini V, Unno W. Theory on non-linear magneto convection and its applications to solar convection problems-I. Publ. Astron Soc., Japan. 1985;37:183-205.
3. Shail R. On laminar two-phase flow in a magnetohydrodynamics. International Journal of Engineering Science. 1973;11:11.3-1108.
4. Lohrasbi J, Sahai V. Magnetohydrodynamic heat transfer in two-phase flow between parallel plates. Applied Scientific Research. 1989;45:53-66.
5. Malashetty MS, Leela V. Magnetohydrodynamic heat transfer in two fluid flow. Proceedings of ASME/AIChE, 27<sup>th</sup> National Heat Transfer conference and Exposition. 1991;28-31.
6. Malashetty MS, Leela V. Magnetohydrodynamic heat transfer in two phase flow. International Journal of Engineering Science. 1992;30:371-377.
7. Linga Raju T, Murty PSR. Hydromagnetic Two-phase flow and heat transfer through two parallel plates in a rotating system. Journal of Indian Academy of Mathematics. 2006;28(2):343-360.
8. Chauhan DS, Rastogi P. Hall current and heat transfer effects on MHD flow in a channel partially filled with a porous medium in a rotating system. Turkish J. Eng. Env. Sci. 2009;33:167-184.
9. Chauhan DS, Rastogi P. Heat transfer effect on rotating MHD couette flow in a channel partially filled by a porous medium with Hall current. Journal of Applied Science and Eng. 2012;15:281-290.
10. Seth GS, Raj Nandkeolyar, Md Ansari S. Hartmann flow in a rotating system in the presence of inclined magnetic field with Hall effects. Tamkang Journal of Science & Engineering. 2010;3:243-252.
11. Linga Raju T, Nagavalli M. MHD two-layered unsteady fluid flow and heat transfer through a horizontal channel between parallel plates in a rotating system. International Journal of Applied mechanics and Engineering. 2014;19(1):97-121.

© 2014 Murty and Prakash; This is an Open Access article distributed under the terms of the Creative Commons Attribution License (<http://creativecommons.org/licenses/by/3.0>), which permits unrestricted use, distribution, and reproduction in any medium, provided the original work is properly cited.

*Peer-review history:*

*The peer review history for this paper can be accessed here:*

<http://www.sciencedomain.org/review-history.php?iid=595&id=33&aid=5635>